

铝合金搅拌摩擦焊时焊接速度与热输入的关系

严 铿，雷艳萍，章 正，方 圆^{*}
(江苏科技大学 先进焊接技术省级重点实验室, 江苏 镇江 212003)

摘 要: 与熔化焊时热输入和焊接速度成反比不同, 搅拌摩擦焊时焊接速度与热输入的关系非常复杂. 文中从摩擦产热和金属塑性变形产热出发, 研究了搅拌摩擦焊时焊接速度与热输入的关系, 以及相同旋转速度与焊接速度比值时焊接速度与性能的关系. 结果表明, 在搅拌摩擦焊时, 焊接速度与热输入不呈线性关系, 而是呈现复杂的形态, 焊接速度在不同的参数范围对热输入的贡献是不同的. 在相同的旋转速度与焊接速度比值时, 随焊接速度的增加, 热输入和接头力学性能的关系也不是线性的. 所以不能用旋转速度与焊接速度的比值来衡量热输入的大小.

关键词: 搅拌摩擦焊; 焊接速度; 热输入

中图分类号: TG456. 9 文献标识码: A 文章编号: 0253-360X(2009)01-0073-04



严 铿

0 序 言

搅拌摩擦焊的焊接原理是利用高速旋转的搅拌工具头插入工件, 由于强烈的摩擦和搅拌, 搅拌头周围的金属迅速被加热; 在旋转搅拌头的临近区域内, 形成了一层充分塑化金属层; 当搅拌头沿着焊件的接缝向前运动时, 在搅拌头的后边就形成了空腔, 由于背面垫板和正面轴肩的密封作用, 在搅拌头转动摩擦力的作用下, 搅拌头前边不断形成的热塑性金属挤压流动, 转移到了搅拌头的后边, 填满了后边的空腔, 空腔的产生与填满几乎同时发生和完成; 这样, 焊缝区的金属被挤压、搅拌, 发生了剧烈的塑性变形, 并被摩擦加热, 在高温中, 原子经过扩散和再结晶, 就形成了搅拌摩擦焊的焊缝. 这就决定了搅拌摩擦焊的产热方式和熔化焊有本质的区别^[1].

在熔化焊时, 热输入是和焊接速度成反比. 而搅拌摩擦焊焊接过程是一个温度变化、组织结构转变、应力应变和金属流动四个因素相互作用的复杂过程^[2]. 其中温度的变化起着主要的作用, 它直接影响到其它因素的改变, 同时它也是其它因素共同作用的结果. 研究搅拌摩擦焊焊接过程中热输入随焊接速度的变化趋势对焊接工艺参数的选择以及焊接中是

否产生缺陷和产生什么样的缺陷有着决定性的作用^[3].

1 试验方法

试验材料为 4 mm 厚的 LF5 铝合金薄板, 尺寸为 300 mm×100 mm. 母材抗拉强度 $R_m \geq 275$ MPa, $R_{p0.2} \geq 145$ MPa, 其化学成分如表 1 所示.

| 表 1 LF5 铝合金母材成分(质量分数, %) | | | | | | |
|--------------------------------------|------|------|-----------|-----------|------|----|
| Table 1 Parent metal elements of LF5 | | | | | | |
| Si | Fe | Cu | Mn | Mg | Zn | Al |
| 0.50 | 0.50 | 0.10 | 0.30~0.60 | 4.80~5.50 | 0.20 | 余量 |

固定旋转速度和搅拌头倾角, 搅拌头尺寸等工艺参数, 仅改变焊接速度, 研究焊接速度对接头性能的影响, 采用的焊接工艺参数如表 2 所示.

| 表 2 改变焊接速度的搅拌摩擦焊工艺参数 | | | |
|---|--------------------------|---|---|
| Table 2 Processing parameter of FSW with changing welding speed | | | |
| 下压量 H/mm | 倾角 $\theta(^{\circ})$ | 焊接速度 $v/(\text{mm}\cdot\text{min}^{-1})$ | 旋转速度 $\omega/(\text{r}\cdot\text{min}^{-1})$ |
| 3.68 | 2.5 | 200~500 | 500 |

2 试验结果与问题

在化学成分固定的情况下, 焊接接头的性能主

收稿日期: 2008-01-04
基金 项目: 江苏省基础研究计划(自然科学基金)资助项目
(BK2008055)
^{*}参加此项工作的还有王陆钊

要取决于焊后的组织状态,而组织状态又主要由冷却速度来决定.冷却速度的大小在散热条件一致的情况下又和焊缝的热输入有密切的关系,也就是说焊接接头的性能与焊接热输入有关.在搅拌摩擦焊条件下如果焊接热输入过小,其热量不足以使焊接区金属达到热塑性状态,因而焊缝成形不好,甚至焊缝表面出现沟槽,强度通常较低.随着焊接热输入的增加,焊缝质量变好,接头强度增加.但是热输入过高,会使焊接区金属过热而导致晶粒长大、焊缝成形及接头质量均变差,因此,在搅拌摩擦焊时通常用焊接接头力学性能的高低和焊接接头断裂的位置来判断搅拌摩擦焊焊接热输入是否合适.

文中在焊接其它参数固定的情况下,测试了 LF5 铝合金搅拌摩擦焊的焊接接头拉伸性能随焊接速度的变换而变化的情况.试验结果如图 1 所示.

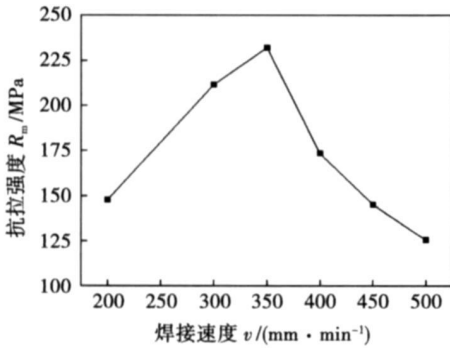


图 1 抗拉强度与焊接速度的关系

Fig. 1 Relation of tensile strength and welding

从图 1 可以看到当焊接速度小于 350 mm/min 时,随焊接速度的增加,抗拉强度增加,当焊接速度为 350 mm/min 时,焊接接头具有最大的抗拉强度.随着焊接速度的继续增加,抗拉强度逐步减小.

在搅拌摩擦焊研究的早期,关于搅拌摩擦焊的产热以及热输入与焊接速度的关系方面还是受熔化焊经典理论的影响.文献[4]认为在搅拌摩擦焊接过程中,在忽略搅拌针旁金属塑性变形热的前提下,焊接接头的力学性能与热输入和材料在搅拌头作用下产生的塑性流变状态有关.搅拌摩擦焊接过程中的焊接热输入可以表示为

$$E = \pi \omega l F (r_0^2 + r_0 r_1 + r_1^2) \left[45 (r_0 + r_1) v \right] \quad (1)$$

式中: ω 为搅拌头的旋转速度, r μm ; μ 为摩擦系数; F 为搅拌头轴肩的压力, N μm ; r_0 为轴肩半径, mm ; r_1 为搅拌针的半径, mm ; v 为焊接速度, $\text{mm} \mu\text{m}$.

由式(1)可知,在搅拌摩擦焊过程中,焊接热输

入的大小取决于搅拌焊头肩部的半径、压力、摩擦系数及旋转转速与焊速之比(n/v).当采用某一搅拌焊头焊接时,其肩部直径为定值,如压力在焊接过程中也保持不变,则焊接热输入仅取决于旋转转速与焊速之比.旋转速度的大小改变了热输入的大小,和热输入成正比,焊接速度的大小在旋转速度一定的情况下与热输入成反比.

但这样的理论无法解释图 1 的试验结果.式(1)中还可以得出一个推论,就是当转速和焊接速度的比值是一个定值时,无论焊接速度是多少,热输入是固定不变的.为了验证这个推论的正确性,还进行了如下的试验.选取焊速为 300, 500, 600 mm/min,同时旋转速度也对应选取 300, 500, 600 r/min,使转速与焊速之比(n/v)为 1.测量当(n/v)为 1 时,不同旋转速度和焊速组合情况下焊接接头的力学性能.结果如图 2 所示.

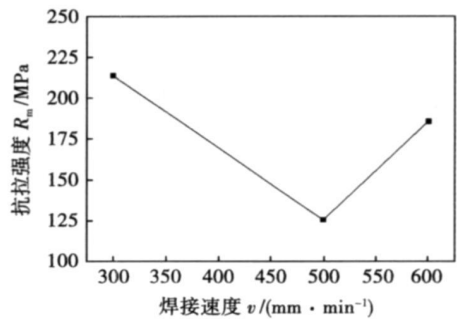


图 2 当(n/v)为 1 时抗拉强度与焊接速度的关系

Fig. 2 Relation of tensile strength and welding speed when (n/v) equal 1

图 2 的试验结果是随不同旋转速度与焊接速度组合的变化,接头强度是变化的,也就是说热输入是变化的,用文献[4]的理论就无法进行解释.在相同的转速下,不同焊接速度以及相同转速前进速度比的焊缝外观形貌如图 3 所示,焊缝的断裂位置如图 4 所示,焊缝的右侧是前进侧.图中 v 代表焊接速度, w 代表旋转速度.

从图 4 中可以看到,焊缝断裂的位置大多位于焊缝中心偏前进侧的地方.这个地方是搅拌摩擦焊焊缝塑性流动最后聚集的地方,如果这时焊接的热量不足,就会在这个地方形成“弱连接”,甚至出现沟槽等缺陷.如果断裂在后退侧,由于后退侧的热量比较高,所以通常是焊接工艺参数偏大,造成晶粒长大所造成的.图 4 也说明了图 1 中焊接接头性能普遍偏低的试验结果.

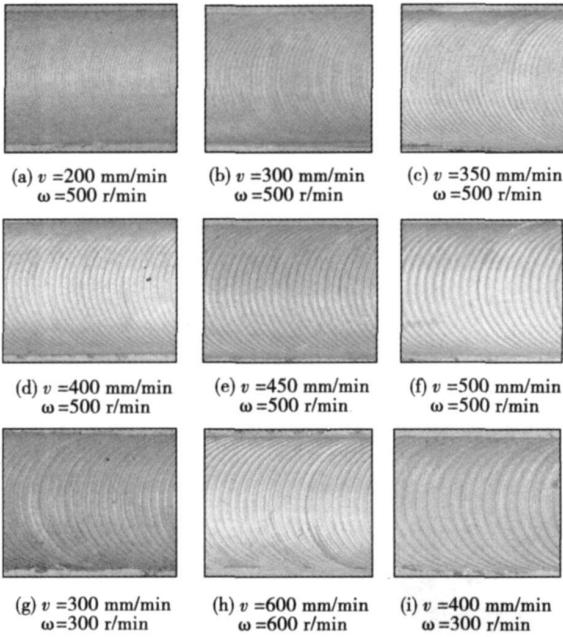


图 3 焊缝外观照片
Fig. 3 Photo of FSW weld

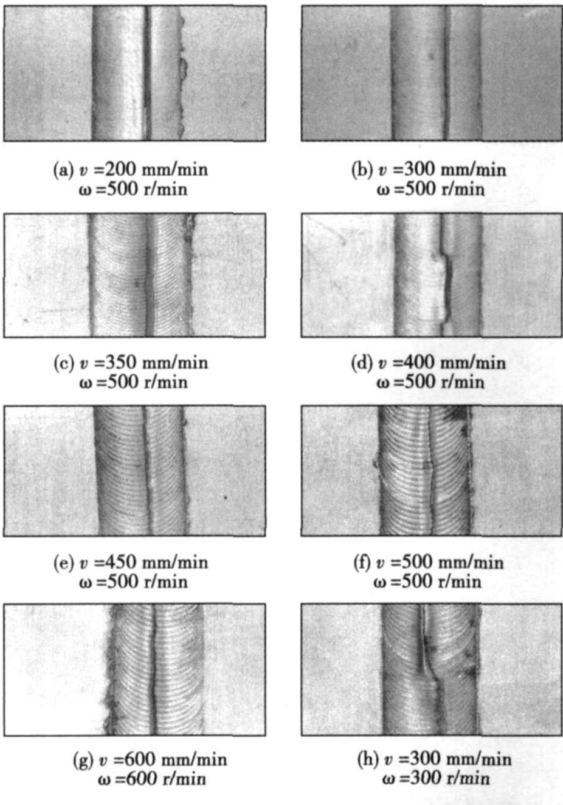


图 4 焊缝断裂位置
Fig. 4 Fracture position of FSW

3 结果分析

结合图 1 和图 2 的试验结果, 可认为搅拌摩擦

焊接过程中的热量来源主要是搅拌头与被焊材料之间的摩擦力做功转化的热量和强烈的塑性变形产生的; 主要的传导介质为被焊材料、搅拌头, 并通过它们的表面与空气的对流而散失热量, 且试板向支撑板传导热量. 热量主要集中于搅拌头和被焊材料相接触摩擦的区域附近, 产热机理不仅与搅拌头轴肩表面形貌有关系, 还与搅拌针的形状有关, 也需要考虑强烈的塑性变形产生的热量.

因此, 在搅拌摩擦过程中, 热输入分两个部分: 轴肩和搅拌针的摩擦产热和金属塑性变形产热. 此时, 与文献[4] 不同的是, 焊接速度与热输入不是简单的反比关系, 搅拌头旋转速度及焊接速度既影响摩擦产热量也对塑性变形热有显著影响. 增加焊接速度从熔化焊的角度是减少了热输入, 因为在熔化焊时产热主要是焊接的电流和电压, 与焊接速度无关. 在搅拌摩擦焊时, 增加焊接速度增加了塑性变形产热, 焊接速度与产热就有一定的函数关系, 但同时焊接速度也和热输入有关系. 所以最终热输入的增减取决于焊接速度引起的塑性变形产热的情况.

搅拌摩擦焊过程中的塑性变形产热主要是因为金属塑性变形“热效应”所致. 一般在较高的速度下使金属塑性变形时, 都有明显的发热现象. 这是因为供给金属产生塑性变形的能量, 消耗在弹性变形和塑性变形上, 耗于弹性变形的能量, 造成物体的应力状态; 而消耗在塑性变形的能量, 因塑性变形的复杂现象(滑移、晶间位错等) 所致, 变形后绝大部分转化为热能, 当这部分热量来不及向外散发而积蓄于物体内部时, 促使温度升高^[5].

搅拌摩擦焊焊接过程中由于搅拌和挤压产生的金属塑性变形非常剧烈, 塑性变形部分远远大于弹性变形部分, 因而可以忽略弹性变形, 将材料模型简化为刚塑性模型, 即搅拌摩擦焊接过程中供给塑性金属变形的能量, 主要转化为热能.

塑性变形过程中的发热现象, 在任何温度下都发生, 不过在低温下表现得明显些, 发出的热量也相对地多些, 因为温度升高时变形抗力降低, 单位变形体积所需要的能量小, 随着温度的升高热效应减小. 这就解释了图 2 的试验结果. 当焊接速度为 300 mm/min 时, 旋转速度只有 300 r/min, 提供的摩擦产热也较小, 温度也较低, 塑性变形发出的热量也相对地多些, 接头性能也较高, 而当焊接速度为 500 mm/min 时, 旋转速度也有 500 r/min, 提供的摩擦产热较大, 温度也较高, 塑性变形发出的热量也相对地少些, 接头性能也就较低. 当焊接速度为 600 mm/min 时, 虽然由于旋转速度较高造成塑性变形发出的热量相对的少些, 但由于旋转速度达到 600 r/min, 提供的摩擦产热较大, 所

以总的热量有所提高, 就造成性能也有所提高。

搅拌摩擦焊的主要工艺参数焊接速度对塑性变形热的影响是通过变形速度加以体现的。焊接速度增大, 变形速度提高, 因而单位时间内的发热量就越多, 同时由于焊接速度的提高热量散发的时间不够, 焊缝的温度升高也越显著。所以, 在焊接速度低于一定的“门槛值”之前, 焊接速度的增大有利于塑性变形热的释放, 促进焊缝成形。

在金属塑性变形过程中, 变形温度对金属的塑性和变形抗力有重大影响。一般情况下, 总的趋势是随着温度升高, 塑性增加, 变形抗力降低。因此, 当温度升高到一定程度时, 焊缝塑性金属变形抗力及单位体积变形功减小, 且高温下热量容易散失, 此时“温度效应”减弱。随着焊接工艺参数的提高, 焊缝温度能够在较短的时间内得到较高的值, “温度效应”减弱, 塑性变形热在整个工艺的热输入中比例下降, 且焊接速度较大对焊缝热输入的减小效果很明显, 塑性变形热不足弥补以因焊接速度提高导致热输入的损失。此时, 过大的提高焊接速度不利于焊缝成形, 容易导致热输入不足, 形成表面沟槽等缺陷。并且由于搅拌头材料的热强性问题, 过大的增加焊接速度, 还将造成搅拌头的断裂^[9]。

综上所述, 焊接速度对热输入的影响可以分为四个阶段。

第一阶段, 焊接速度过小, 塑性变形产热忽略不计, 主要的产热是摩擦产热。由于热输入过大, 造成焊缝的晶粒长大, 力学性能下降。随焊接速度的增加, 热输入趋向合理, 这时力学性能提高, 并达到最大值。

第二阶段, 当焊接速度不是很大时, 塑性变形产热不明显, 随焊接速度的增大, 塑性变形热在焊缝热输入中所占的比例逐步提高, 但塑性变形增加的热量小于焊接速度增加减少的热输入。所以总体上这个阶段是随焊接速度的增加, 热输入下降, 焊接接头的力学性能也下降, 并降到最低点。

第三阶段, 当焊接速度超过一定的值时, 塑性变形热在焊缝热输入中所占的比例增加, 塑性变形增加的热量大于焊接速度增加减少的热输入。所以总体上这个阶段是随焊接速度的增加, 热输入增加, 焊接接头的力学性能上升, 并达到阶段最高点。

第四阶段, 由于焊接速度过快, 塑性变形热和摩擦产热来不及进行热传导, 造成焊缝上下层热量不均匀, 总体上这个阶段是随焊接速度的增加, 热输入

减少, 焊接接头的力学性能下降, 继续增加焊接速度, 由于搅拌头热强性的问题, 发生搅拌头剪切断裂。

4 结 论

(1) 在搅拌摩擦焊时, 焊接速度与热输入不呈线性关系, 而是呈现复杂的形态。当焊接速度较小, 塑性变形产热可以忽略时, 摩擦热占主要地位。这时随焊接速度的增加, 热输入减小, 接头性能下降。当焊接速度较大, 塑性变形产热占主要地位时, 随焊接速度的增加, 热输入增加, 接头性能上升。当进一步增加焊接速度, 由塑性变形引起的产热小于焊接速度增加造成的热输入减小, 总的热输入减小, 性能下降。

(2) 当旋转速度与焊接速度比值为定值时, 接头力学性能是变化的, 并且不是线性的。由摩擦热、塑性变形产热综合影响接头的性能。摩擦热是随旋转速度和焊接速度的绝对值的增加而增加, 塑性变形热是先下降后上升, 总的趋势是先下降, 后上升。

参考文献:

- [1] McClure J C. A thermal model of friction stir welding[J]. Trends in Welding Research, 1999, 62(5): 25—29.
- [2] Song M, Kovacevic R. Thermal modeling of friction stir welding in a moving coordinate system and its validation[J]. Machine Tools and Manufacture, 2003(43): 605—615.
- [3] 栾国红, North T H, 郭德伦, 等. 铝合金搅拌摩擦焊接头行为分析[J]. 焊接学报, 2002, 23(6): 62—66.
Luan Guohong, North T H, Guo Delun, et al. Characterizations of friction stir welding on aluminum alloy[J]. Transactions of the China Welding Institution, 2002, 23(6): 62—66.
- [4] 汪建华, 姚 舜, 魏良武, 等. 搅拌摩擦焊焊接的传热和力学计算模型[J]. 焊接学报, 2000, 21(4): 61—64.
Wang Jianhua, Yao Shun, Wei Liangwu, et al. Thermal and thermo-mechanical modeling of friction stir welding[J]. Transactions of the China Welding Institution, 2000, 21(4): 61—64.
- [5] 彭大暑. 金属塑性加工原理[M]. 长沙: 中南大学出版社, 2004.
- [6] 聂 洁. 铝合金厚板搅拌摩擦焊工艺研究[D]. 镇江: 江苏科技大学, 2008.

作者简介: 严 铿, 男, 1961 年出生, 教授, 硕士研究生导师。主要从事焊接新工艺和搅拌摩擦焊工艺研究, 获得国家科技进步三等奖 1 项, 省部级奖 8 项。发表论文 40 余篇。

Email: yankeng@126.com

lyre commended.

Key words: laser cladding; multiple linear regression; genetic neural network; prediction of the form; comparative analysis

Effect of gallium on microstructure and properties of Ag-Cu-Zn filler metal LU Fangyan¹, XUE Songbai¹, LAI Zhongmin^{1,2}, ZHANG liang¹, GU Liyong³, GU Wenhua³ (1. Nanjing University of Aeronautics and Astronautics, Nanjing 210016, China; 2. Jiangsu University of Science and Technology, Zhenjiang 212003, Jiangsu, China; 3. Changshu Huayin Filler Metals Co. Ltd., Changshu 215513, Jiangsu, China). p55—59

Abstract: Melting temperature, spreadability, microstructures of silver filler metal with different content of gallium, and the mechanical properties of brazed joints were studied respectively. Results show that adding gallium can decrease the melting temperature, improve the spreadability of the silver filler metal, and the microstructure of the silver filler metal was refined significantly. Using copper and brass plates as base metal, brazing with flame method, the mechanical properties of the joints brazed with lap joint and butt joint were tested and analyzed at the same time. Results indicate that the fracture position of two kinds of brazed joints happened on the base metal, except for the lap joint of brass, which shows better mechanical properties of the joints brazed with the silver filler metal bearing gallium. For the lap joint of brass, the tensile strength gradually strengthened with the increasing of gallium content, and the optimum content of Ga causing best comprehensive properties of the AgCuZn filler metal is about 3.0%.

Key words: silver filler metal; melting temperature; spreadability; microstructure; mechanical properties

Porosity formation mechanisms and controlling technique for laser penetration welding of aluminum alloy GONG Shuili¹, YAO Wei¹, Steve Shi² (1. National Key Laboratory for High Energy Density Beam Processing Technology, Beijing Aeronautical Manufacturing Technology Research Institute, Beijing 100024, China; 2. TWI Ltd, Cambridge CB1 6AL, United Kingdom). p60—62

Abstract: The distribution and appearance characteristics of porosities in laser penetrated weld of aluminum alloy were observed, the formation mechanisms of porosities were analyzed in detail, and the influences of twin-spot laser energy distribution on porosities were investigated. It showed that there are two kinds of porosities, metallurgical and technologic porosities in laser penetrated weld of aluminum alloy. The formation of metallurgical porosities is related to the separation, congregation and incorporation of hydrogen in the weld pool, while instantaneous instability of its keyhole is an essential reason for the occurrence of technologic porosities. Twin spot laser energy distribution can enlarge diameters of the opening and the root of its keyhole, improve fluctuating conditions of the wall of its keyhole, increase stability, and consequently decrease technologic porosities in number, but it has no obvious influence on metallurgical por-

osities.

Key words: laser penetration welding; porosity; twin spot; aluminum alloy

Development of duplex stainless steel flux-cored wire GDQA2205 LI Wei, LI Zhuoxin, LI Guodong, LI Hui (Department of Material Science and Engineering, Beijing University of Technology Beijing 100124, China). p63—67

Abstract: The developed wires were used for gas metal arc welding. The chemical composition, microstructure, tensile strength and corrosive pitting rate of weld bead and Rockwell hardness, bend strength and impact toughness of welded joint were investigated. The microstructure of weld metal was analyzed by metalloscope. The impact fracture was analyzed by scanning electron microscope, and inclusions of impact fracture were analyzed by energy spectrometer. Experiment results indicated that it was effective to add rational nickel and Mn in the wire to accelerate austenite formation. The influence factors of pitting corrosion resistance and impact ductility were studied. It had been found that, besides chemical constitution, the uniform distribution of duplex phases in the weld metal could improve pitting corrosion resistance. Elements Mn, Ni, Cr etc. were the assurance of welded joint impact ductility.

Key words: duplex stainless steel; flux-cored wire; weld; joint performance

Image processing of weld seam based on beamlet transform DENG Shuangcheng¹, JIANG Lipai¹, JIAO Xiangdong¹, XUE Long¹, DENG Xiabin² (1. Opto-Mechatronic Equipment Technology Beijing Area Major Laboratory, Beijing Institute of Petrochemical Technology, Beijing 102617, China; 2. Beijing Spacecrafts, China Academy of Space Technology, Beijing 100080, China). p68—72

Abstract: A novel algorithm based on beamlet transform for detecting weld seam edges was presented. Taking into account of some special characteristics of welding image processing, an orientation-thresholding step as well as a two-scan method to the standard beamlet-based line detection algorithm were introduced. Experiments are conducted to detect weld seam edges in noisy weld seam images to test the anti-noising performance of the algorithm. The result of experiments show that the algorithm is capable of directly extracting weld seam edges from highly noisy weld seam images without any pre-processing or post-processing steps, showing its high efficiency and prominent anti-noising performance. The two-scan method is particularly helpful when coping with low SNR weld seam images.

Key words: beamlet transform; weld seam; image processing; line detection

Relation of welding speed and heat input at aluminum alloy friction stir welding YAN Keng, LEI Yanping, ZHANG Zhen, FANG Yuan, WANG Luzao (Provincial key Lab of Advanced Welding Technology, Jiangsu University of Science and Technology,

Zhenjiang 212003 Jiangsu, China). p73—76

Abstract Different from the relationship of heat input and welding speed at melting welding, which submits inverse ratio, the relation is quite complex for friction stir welding. This paper studies the relation of welding speed and heat input at aluminum alloy friction stir welding based on thermogenesis of friction and plastic deforming. The result shows that welding speed and heat input relationship is nonlinear and shows a complex shape, which means welding speed, depending on various ranges of parameter, contributes variably to heat input. When rotary speed to welding speed ratio is constant, with the increase of welding speed, heat input and the mechanical behavior of the joint decreasing is not linear. Thus, heat input should not be measured by rotary speed to welding speed ratio.

Key words: friction stir welding; welding speed; heat input

Interface microstructure and wear properties of TiC-Ni-Mo coatings prepared by in-situ fabrication of laser cladding HE Qingkun, WANG Yong, ZHAO Weimin, CHENG Yiyuan (College of Mechanical and Electronic Engineering, China Petroleum University, Dongying 257061, Shandong China). p77—80, 100

Abstract: TiC-Ni-Mo composite coating was prepared by in-situ fabrication of laser cladding. The interface microstructure and wear properties of the coating was investigated by means of EPMA, TEM and wear tests. The results show that adding 5% Mo into the coating could improve uniformity, rigidity, wear resistance, refine TiC grains, reduce friction coefficients and exist orientation relationship: $(001)_{\text{TiC}} // (1\bar{1}1)_{\gamma\text{-Ni}}$. The rigidity and wear resistance of coating decrease with the content of 10 % Mo. There are many directional dislocations inside TiC phase and dislocation tangles inside γ -Ni binder phase. The wear mechanism of the coating is anti-wear action of reinforcing phases. The wear morphology is short and shallow furrows.

Key words: laser cladding; in-situ fabrication; interface; wear resistance

Study on welded metal properties of high carbon cast self-shielded flux cored wire with Nb and Mo WANG Qingbao¹, BAI Bo¹, LIU Jingfeng¹, LIAN Jing² (1. Welding Research Institute, Central Research Institute Building & Construction, MCC, Beijing 100088, China; 2. Heilongjiang Provincial Installation Engineering Company, Harbin 150000, China). p81—84

Abstract: The paper studied the microstructures morphology, and the discrimination in hardness and wearability of welded metal with the addition of Nb, Mo by optical microscope and SEM. The results showed that the number of primary carbide, macrohardness and wearability were increased with the increasing the contents of Nb, Mo. Nb only resulted in NbC to strength welded metal, and but this strengthen was better; Mo not only resulted in Mo₂C but also in the primary carbide and matrix, but this strengthen was weaker than that

of Nb. In order to get better wear resistance and economic benefit, it should optimize the contents of alloys and strengthen both carbide and matrix.

Key word primary carbide; strengthen; matrix; wearability

Experimental study on compression-diffusion composite connection of Cu/Al joint HONG Liling, XIN Xuanrong, ZHANG Keke, LIU Ting, WANG Wenyao (School of Materials Science and Engineering, Henan University of Science and Technology, Luoyang 471003, Henan China). p85—88

Abstracts: Cu and Al alloy were bonded by compression-diffusion composite connection technology. The welding technics procedure was: Cu and Al alloy be compressed firstly, then diffused on 515 °C for 60 min, and diffused 90 min again before hot-pressed. The microstructure was researched by various test methods, such as SEM, EDS, micro-hardness test, XRD and so on. The experiment results indicated that brittle compound CuAl₂ appeared in the interface and a new component was created between Cu & welding which looks like a bright belt. Electric performance of joint was between Cu and Al alloy, that could be satisfied with practical application.

Key words: compression-diffusion composite connection; copper; aluminum alloy; weld

Finite element simulation of temperature field for submerged arc strip overlaying on thick plate WANG Zhifeng¹, CHEN Peiyin¹, WU Wei¹, CHEN Yan¹, ZHANG Jianmin², Bao Heng² (1. Harbin Welding Institute, Harbin, 150080, China; 2. China First Heavy Industries, Qiqihar 161042, Heilongjiang China). p89—92

Abstract: A thermal source for submerged arc overlaying is designed based on its principle and heat source model of Goldak, and a fortran subroutine is compiled to implement the translation of thermal source in the FEA software MSC. MARC. Finite element simulation of temperature field of submerged arc strip overlaying on thick plate was established. The simulation results are in good accordance with the actual thermal cycle curve, which proved the model is correct.

Key words: submergen arc overlay welding; heat source model; heat source temperature field; thermal cycle curve

Oxidation resistance of reactive plasma cladding high-chromium iron-base composite coating WANG Limei (School of Information and Control Engineering, Weifang University, Weifang 261061, Shandong China). p93—95, 104

Abstract The sucrose was used as a carbonaceous precursor to prepare composite powders of Fe-Cr-C-W-Ni by the precursor carbonization-composition process. And the powders were fused to form a high-chromium iron-base coating on the surface of hardened and tempered grade C steel ($C \leq 0.35\%$) with the optimum reactive plasma cladding process. SEM, XRD and EDS were employed to